

OVERALL INJECTION STRATEGY FOR FCC-ee

S. Ogur ^{*†}, F. Antoniou, T. K. Charles [‡], O. Etisken [§], B. Harer, B. Holzer, K. Oide [¶],
 T. Tydecks, Y. Papaphilippou, L. Rinolfi, F. Zimmermann, CERN, Geneva, Switzerland,
 A. Barnyakov, A. Levichev, P. Martyshkin, D. Nikiforov, BINP SB RAS, Novosibirsk, Russia,
 E. V. Ozcan, Bogazici University, Bebek, Istanbul, Turkey,
 K. Furukawa, N. Iida, T. Kamitani, F. Miyahara, KEK, Tsukuba, Ibaraki, Japan,
 I. Chaikovska, R. Chehab, LAL, Orsay, Paris, France,
 S. M. Polozov MEPhI, Moscow, Russia, M. Aiba, PSI, Zurich, Switzerland.

Abstract

The Future Circular electron-positron Collider (FCC-ee) requires fast cycling injectors with very low extraction emittances to provide and maintain extreme luminosities at center of mass energy varying between 91.2-385 GeV in the collider. For this reason, the whole injector complex table is prepared by putting into consideration the minimum fill time from scratch, bootstrapping, transmission efficiency as well as store time of the beams in synchrotrons to approach equilibrium emittances. The current injector baseline contains 6 GeV S-band linac, a damping ring at 1.54 GeV, a pre-booster to accelerate from 6 to 20 GeV, which is followed by 98-km top up booster accelerating up to final collision energies. Acceleration from 6 GeV to 20 GeV can be provided either by Super Proton Synchrotron (SPS) of CERN or a new synchrotron or C-Band linac, distinctively, which all options are retained. In this paper, the current status of the whole FCC-ee injector complex and injection strategies are discussed.

INTRODUCTION

The Future Circular electron-positron Collider (FCC-ee) is designed to provide precision study of Z , W , H bosons and top quark, as a potential first step to the global FCC project of CERN. In 98 km collider, these 4 particles will be studied in 4 different operational modes within the distinct time intervals (i.e. upgrades) of the collider [1].

The injector complex consists of a linac, damping ring, pre-booster and top-up booster, as presented in Fig. 1. Inevitably, this chain requires scheduling of bunches in order to fill the collider within minimum time meanwhile allocating enough time to the beams to approach to the equilibrium emittances of the circular accelerator for their stabilisation before the energy ramp up. On the other hand, the injector complex will have the one tenth of the bucket charge in the collider on average, therefore while topping up into the same collider bucket, we have needed to investigate the fluctuations of the bunch length as well as transverse emittances due to beamstrahlung, also known as boothstrapping [2]. The injection into the proceeding synchrotron (for example

from SPS to top-up booster) is also an important limiting parameter to the synchrotrons determining the required dynamic aperture as well as to the spacing between the bunches or the trains. In Table 1, the injection types have been tabulated. All in all, the FCC-ee injector complex will provide the necessary beams with the same accelerators yet distinct cycles as discussed in details in Table 2.

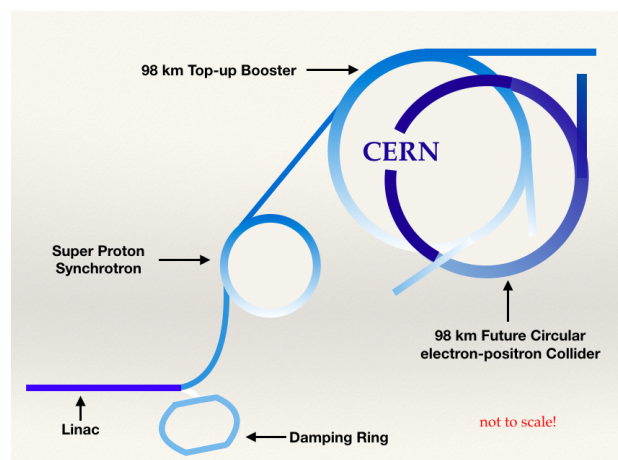


Figure 1: Layout of the FCC-ee.

Table 1: Injection types into the circular accelerators

accelerator	injection type
damping ring	on axis
pre-booster	off-axis
top-up booster	on-axis
collider	off-axis

ELECTRON AND POSITRON PRODUCTION

A low emittance RF-gun has been considered in order to preserve beam transmission and prevent emittance dilution due to wakefields throughout the injector complex. The novel RF-Gun operating at 2856 MHz frequency has been designed to provide 6.5 nC charge in a bunch with

* salim.ogur@cern.ch

† also Bogazici University, Bebek, Istanbul, Turkey

‡ also School of Physics, University of Melbourne, 3010, Victoria, Australia

§ also Ankara University, Ankara, Turkey

¶ also KEK, Tsukuba, Ibaraki, Japan

Table 2: Baseline parameters for the FCC-ee injectors

operation mode	FCCee-Z		FCCee-W		FCCee-H		FCCee-tt	
	Full	Top-up	Full	Top-up	Full	Top-up	Full	Top-up
type of filling	Full	Top-up	Full	Top-up	Full	Top-up	Full	Top-up
energy [GeV]	45.6		80		120		182.5	
lifetime [min]	70	70	50	50	42	42	47	47
τ_{inj} [sec]	122	122	44	44	31	31	32	32
linac bunches	2	2	2	2	1	1	1	1
linac repetition rate [Hz]	200	200	100	100	100	100	100	100
linac RF frequency [MHz]	2856							
linac bunch population [10^{10}]	2.13	1.06	1.88	0.56	1.88	0.56	1.38	0.83
SPS bunch spacing [MHz]	400							
SPS bunches/injection	2	2	2	2	1	1	1	1
SPS bunch population [10^{10}]	2.13	1.06	1.88	0.56	1.88	0.56	1.38	0.83
number of linac injections	1040	1040	500	500	393	393	50	50
number of SPS injections	8	8	2	2	1	1	1	1
SPS supercycle duty factor	0.84	0.84	0.62	0.62	0.35	0.35	0.08	0.08
SPS number of bunches	2080	2080	1000	1000	393	393	50	50
SPS current [mA]	307.15	153.57	130.22	39.07	51.18	15.35	4.77	2.86
SPS injection time [s]	5.9	5.9	5.7	5.7	3.93	3.93	0.5	0.5
SPS ramp time [s]	0.2							
SPS cycle length [s]	6.3	6.3	6.1	6.1	4.33	4.33	0.9	0.9
BR bunch spacing [MHz]	400	400	400	400	400	400	400	400
BR number of bunches	16640	16640	2000	2000	393	393	50	50
BR bunch population [10^{11}]	0.21	0.11	0.19	0.06	0.19	0.06	0.14	0.66
BR cycle time [s]	51.74	51.74	14.4	14.4	7.53	7.53	5.6	5.6
booster ramp time	0.32	0.32	0.75	0.75	1.25	1.25	2	2
number of cycles per species	10	1	10	1	10	1	20	1
transfer efficiency	0.8							
no. of injections/collider bucket	10	1	10	1	10	1	20	1
total number of bunches	16640	16640	2000	2000	393	393	50	50
filling time (both species) [sec]	1034.8	103.48	288	28.8	150.6	15.06	224	11.2
required bunch population [10^{11}]	1.70	0.085	1.5	0.045	1.5	0.045	2.2	0.066

the normalised transverse emittance of $3 \mu m^1$, and $\sigma_z = 1.5$ mm bunch length with 0.6% energy spread at 10 MeV. The designed RF-Gun [3,4] is shown in Fig. 2.

Apart from RF gun, a thermionic gun will also be utilized in order to supply 10 nC of bunch charge. Actually, the whole injector complex is designed to accelerate 3.4 nC (i.e. 2.13×10^{10}) electron or positron in a bunch or bucket, the charge extracted from the electron sources are intentionally designed to be higher in order to have safety margins for unforeseen transmission loss, positron production, last but not least, to be able to send higher charge for the first fill of the collider.

The creation of the positrons will be done by impinging electrons on a target inside the linac at 4.46 GeV. Regarding the probable transmission loss in the capture and acceleration of positrons inside the remaining 1.54 GeV part of the linac, some safety margin is allocated for the incident electron charge into the positron target. In other words, the FCC-ee injectors can impinge the target with up to 10 nC of

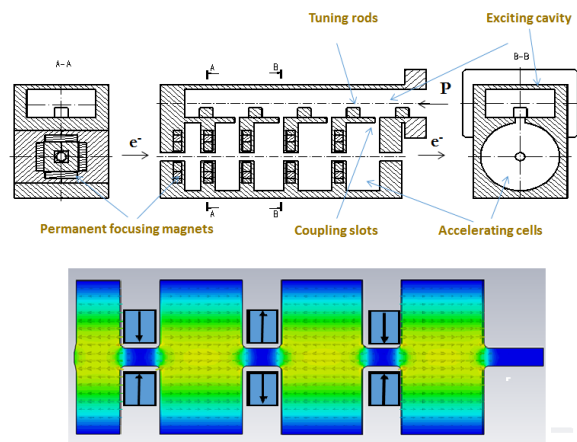


Figure 2: Sketch of S-Band RF-gun using parallel coupling accelerating structures with permanent magnets in the irises and its corresponding electromagnetic simulations.

electron bunch at 4.46 GeV in order to achieve 3.4 nC of positrons at 1.54 GeV at the end of 6 GeV linac. The target

¹ Instead of π .mm.mrad, the unit of the emittance is said to be μm , and this notation is followed through the paper.

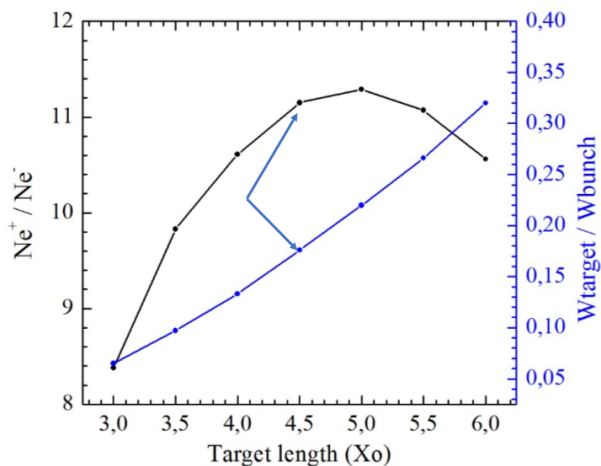


Figure 3: Optimisation of conventional positron target thickness with positron yield (left vertical axis), and total energy deposition in tungsten target is normalised by the total electron bunch energy (right vertical axis).

simulations are retained for both conventional and hybrid targets [5]. In Fig. 3, the conventional target length versus positron production yield has been presented, and the target thickness would suffice the FCC-ee needs determined to be 16 mm thick tungsten foil where the tungsten radiation length is denoted as X_0 corresponding to 3.5 cm. The power deposited in the target is calculated to be 2.8 kW per pulse. For max e^- charge of 8.8 nC (i.e. net of transmission loss out of 10 nC e^- in a bunch sent from the thermionic gun), e^- beam energy is 76 J (2 bunches per RF pulse with 200 Hz of linac repetition), in other words, the average e^- beam power on the target is 15 kW [6].

The optimisation of positron targets, flux concentrator as well as accelerating structures surrounded by the solenoids and triplets are currently on going [7, 8]. Meanwhile, the e^+ beam used in the FCC-ee injector simulations are taken from KEK, which the positrons simulated from the conversion target up to 1.1 GeV in the linac [9].

LINACS

6 GeV S-Band linac operating at 2856 GHz has been finalised excluding positron optics. The linac has a branching point at 1.54 GeV for emittance cooling in the damping ring. The space charge in the RF gun as well as in the first 75 MeV part of the linac have been taking into account (i.e. up to 85 MeV). The misalignments have been randomly distributed and the automatic orbit steering algorithm has successfully transmitted the beam with transverse emittance dilution below 15% with perfect transmission, leaving more than an order of magnitude safety margin for the injected emittance into the pre-booster. The linac basics and former versions have been already presented in [10], yet some modifications and updates have been done and presented in this chapter.

The 1.54 GeV electrons will be injected into damping ring (DR) for 25 ms, and then injected back to the linac after

emittance cooling via a bunch compressor (BC), which DR and BC will be discussed in the following sections. Therefore, the linac is continued from 1.54 GeV up to 6 GeV using S-Band cavities, where its optics and some parameters are presented in Fig. 4 and Table 3, respectively.

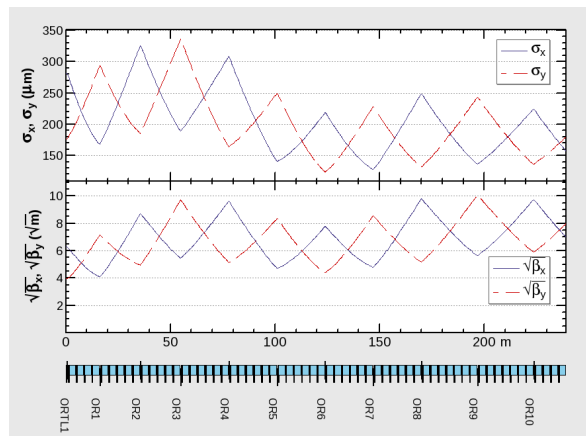


Figure 4: Optics of 1.54-6 GeV linac.

Table 3: Some parameters of the 1.54-6 GeV linac.

Parameter	Value
length	239.1 m
frequency	2856 Hz
repetition	200 Hz
number of bunches per RF pulse	2-4
number of quad./cavity	12, 60
injection-extraction energy	1.54 GeV-6 GeV
injected emittance (h/v)	1.86/0.39 nm
average extracted emit. (h/v)	0.55/0.11 nm
final emittance w/o blowup (h/v)	0.48/0.10 nm
transmission for 3.4 nC	100%

The 6 GeV linac will accelerate both beams alternatively. During the electron beam delivery into boosters, the linac will send 2 bunches per RF pulse, however, during positron beam creation, there will be 2 e^+ bunches followed by 2 high charge e^- up to 4.46 GeV part of the linac to create new positron bunches which will be sent into the DR.

The FCC-ee injector baseline foresees utilisation of the CERN SPS or a new synchrotron as a pre-booster. On the other hand, high gradient C-Band linac can be also a compelling alternative for 6-20 GeV acceleration interval. The C-Band accelerating structures of 1.8 m length will have an aperture of 16 mm with 50 MV/m unloaded cavity gradient. The main parameter of the C-Band linac has been given in Table 4. The short-range wakefields [11] have been included in the simulations together with misalignments of quadrupoles and cavities, misinjection, and BPM readout errors, as in the case of S-Band linac. The optics of C-Band cavities is preceded by the S-Band 1.54-6 GeV linac in Fig. 4, and therefore it continues starting from the 'QC0' quadrupole in Fig. 5.

Content from this work may be used under the terms of the CC BY 3.0 licence (© 2018). Any distribution of this work must maintain attribution to the author(s), title of the work, publisher, and DOI.

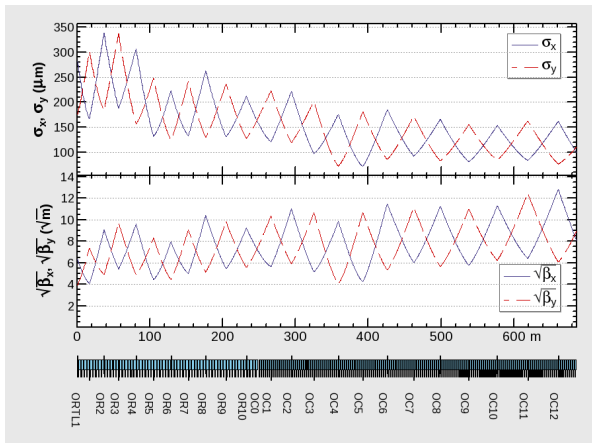


Figure 5: Optics of 1.54-20 GeV linac. Note that C-Band accelerating structures starts at 'QC0' after S-Band structures.

Table 4: Some parameters of the C-Band 6-20 GeV linac

Parameter	Value
length	446.9 m
frequency	5712 Hz
repetition	200 Hz
number of bunches per RF pulse	2
number of quad./cavity	13, 156
average extracted emit. (h/v)	1.18/0.05 nm
final emittance w/o blowup (x/y)	0.15/0.03 nm
transmission for 3.4 nC	100%

C-Band structure has brought 447 meter additional length to S-Band 6 GeV linac in order to reach 20 GeV. Moreover, the extracted emittance values 1.18/0.05 nm, which are calculated for 12 random seeds, are quite compatible with the injection emittance to the booster. Moreover, thanks to utilisation of DR for emittance cooling of both species, the energy spread of the beams at 20 GeV is around $\pm 0.7\%$ in total, allowing safe direct injection into the top-up booster, as the beam profile of tracking can be seen in Fig. 6.

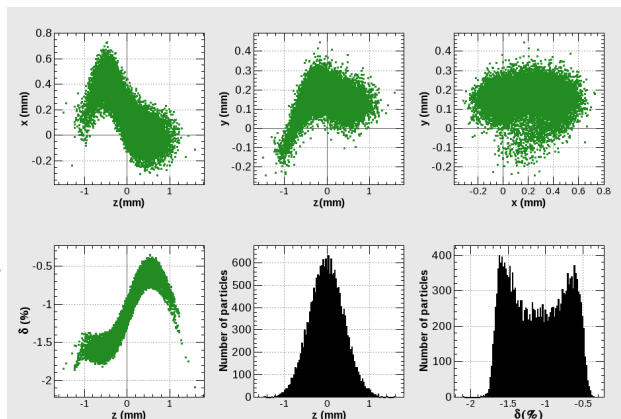


Figure 6: Beam profile at the end of S-Band plus C-Band linac at 20 GeV

DAMPING RING

The primary intend of using damping ring for FCC-ee is the emittance cooling of the positrons, yet for the compatibility of both species, the DR is planned to be used for the e^- beam as well without bringing any additional delay to the e^- beam delivery to the collider. The damping ring is designed to be at least 240 meter (i.e. about 800 ns for relativistic $\beta \approx 1$) in order to be able to host 5 trains separated by 100 ns due to kicker rise/fall times, and each train has 2 bunches RF pulse coming from linac separated by approximately 60 ns due to long range longitudinal wakes, as discussed in details in [10]. The DR optics has been changed slightly to mitigate the impact of Intra-beam scattering (IBS), which is done by creating 20% x-y coupling in the optics. The optics have been shown in Fig. 7 and some corresponding parameters of DR is tabulated in Table 5.

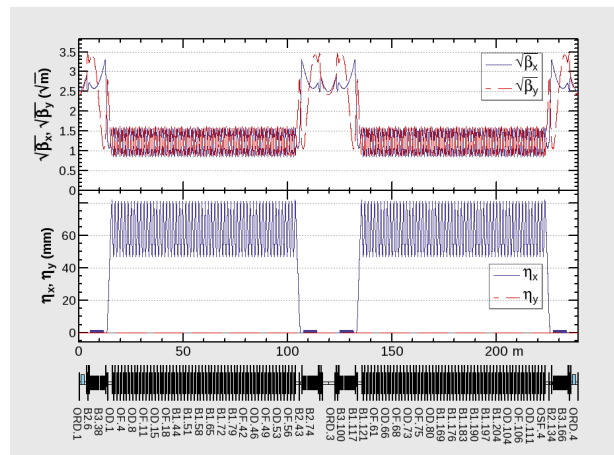


Figure 7: Damping ring optics.

Table 5: 1.54 GeV damping ring parameters with IBS and 20% coupling

parameter	value
circumference	241.8 m
bending radius	7.75 m
no. trains, bunches/train	5, 2
train, and bunch spacings	100 ns, 61 ns
FODO cell phase advance (h/v)	69.5/66.1 deg
betatron tune (h/v)	24.19/23.58
equilibrium emittance (h/v)	1.38/0.28 nm
longitudinal equilibrium emittance	1.73 micrometers
damping time (h/v/l)	10.5/10.9/5.5 ms
no. of wigglers, theirs fields	4, 1.8 T
energy loss per turn	0.23 MeV
RF voltage, frequency	4 MV, 400 MHz

The dynamic aperture(DA) of the DR has been calculated to be around $\pm 7\%$, therefore it rules out usage of an energy compressor since the positrons have an energy spread of $\pm 5\%$ after the collimation of the long tail particles. Therefore, they can be injected into the DR directly by a mere transverse

matching. The DA achieved in transverse and longitudinal directions is shown in Fig. 8.

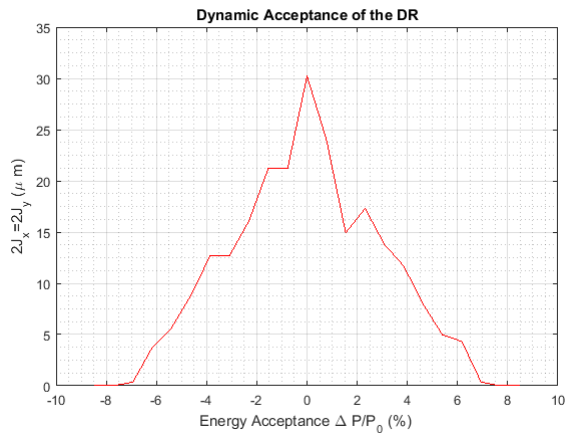


Figure 8: Dynamic acceptance for 1000 turns with synchrotron radiation.

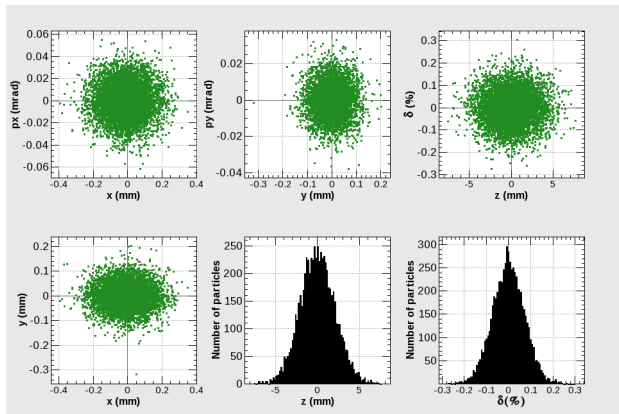


Figure 9: Positron beam profiles after tracking in the ideal DR for the allocated beam store time of 45 ms.

All in all, the DR tracking results are outstandingly close to the analytic calculations and equilibrium emittance of the DR, as presented in Table 6.

Table 6: DR tracking results of positron beam for 45 ms in the ideal machine with 20% coupling to mitigate IBS

direction	injected emittance	extracted emittance
horizontal	1.26 μm	1.48 nm
vertical	1.21 μm	0.38 nm
longitudinal	75.5 μm	1.48 μm

However, a bunch compressor after DR is required to reduce the RMS bunch length from 5 mm (assuming the cavity voltage of the DR is reduced in order to prevent CSR kick, actually $\sigma_z=2.2$ mm in Fig. 9) to 0.5 mm, prior to injection into the linac. A dogleg bunch compressor comprised of two

triple bend achromat (TBAs) can achieve this compression. The full details of which can be found in [12].

The longitudinal dispersion properties of the bunch compressor are: $R_{56} = 0.40$ m, $T_{566} = 61.8$ mm, and $U_{5666} = -23.5$ mm, where T_{566} and U_{5666} are the second- and third-order longitudinal dispersion respectively. Sextupole magnets placed in the dispersive region not only optimize of the second-order longitudinal dispersion, T_{566} , to linearize the longitudinal phase space distribution, but also correction the chromaticity.

Left unchecked, CSR has the potential to significantly degrade the quality of the beam. This is true despite the relatively long bunch length ($\sigma_{z,f} = 0.5$ mm) because the reasonably large R_{56} value required necessitates a large degree of bending. Fortunately, CSR cancellation techniques [12–17] can mitigate the emittance growth to an acceptable level (less than 10%). Careful control of β_x and α_x at the center of each dipole, as well as the phase advance between each dipole can allow us to cancel out the CSR kicks (Δx_k and $\Delta x'_k$) almost completely. To compensate for the CSR kicks, an additional quadrupole magnet is needed in the section between the TBAs. Figure 10 compares of the emittance growth through the bunch compressor when this CSR kick analysis is applied and when it is not.

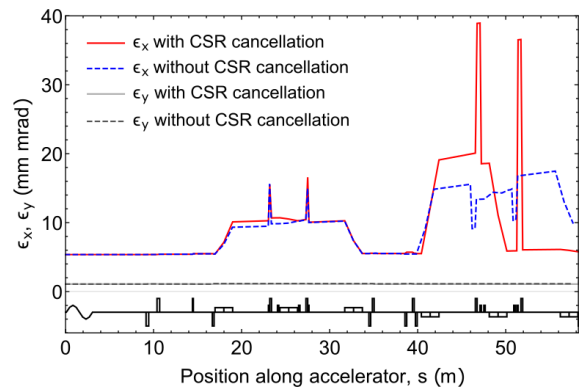


Figure 10: Emittance along the bunch compressor, before CSR cancellation technique applies (blue, dotted) and after (red, solid).

The positron beam of KEK has been simulated through matching section to the DR, 45 ms in the DR, then these particles are gone through BC, finally another matching has been done to the linac at 1.54 GeV. This overall tracked beam has been used in Linac simulations presented in the former chapter.

PRE-BOOSTERS

Two different options are considered as a pre-booster before the bunches transferred to the high-energy booster: using the existing Super Proton Synchrotron (SPS) or designing completely a new ring. The initial basic parameters for the FCC-ee pre-injector were established in order to satisfy the collider flux requirements and using the CERN SPS as

Content from this work may be used under the terms of the CC BY 3.0 licence (© 2018). Any distribution of this work must maintain attribution to the author(s), title of the work, publisher, and DOI.

a pre-booster ring (PBR) [18]. Since there can be issues on using the SPS as pre-injector due to machine availability, synchrotron radiation and RF system requirements, a "green field" alternative pre-booster ring design is also considered [19]. The purpose of this study is to present the necessary modifications on the existing SPS and the conceptual design of an alternative accelerator ring with injection and extraction energies of 6 and 20 GeV, respectively.

SPS as Pre-booster

Damping wiggler and Robinson wiggler magnets are proposed to be installed in the straight sections of the SPS, in order to achieve the required emittance like in the case of the CLIC damping rings design [20].

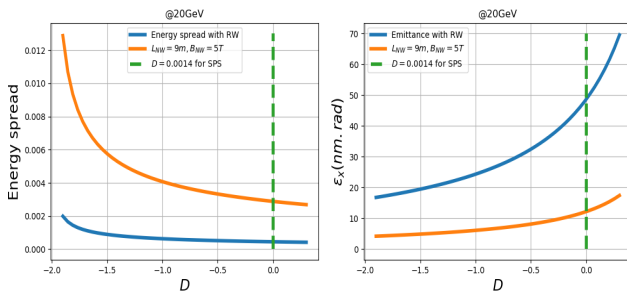


Figure 11: Parametrization of the energy spread (left) and emittance (right) with the normal wiggler (NW) and Robinson wiggler (RW) magnet at 20 GeV for SPS

For the existing SPS, the achievable emittance and damping time are around 48 nm and 1.7 s, respectively, even if the phase advance for one FODO cell is arranged to around 135 degree. However, the horizontal emittance can be significantly decreased by adding a Robinson wiggler yet it introduces a growth in the energy spread [21–23], as it can be seen in Fig. 11. The preliminary results have concluded the emittance to be reduced to 12 nm from around 48 nm by deploying damping wiggler magnet with 9 m and 5 T. Then, the emittance is further reduced to required 5 nm by introducing a Robinson wiggler. In conclusion, the damping time becomes much lower than the required 0.1 s thanks to these proposed wiggler magnets.

Alternative Ring Design

The structure of alternative ring has been provided based on the analytic calculations and simulations. A FODO type cell is chosen for the ring which has 4 arcs and 4 straight sections. Wiggler magnets are planned to be placed in one of the straight sections to be able to have 0.1 s damping time at 6 GeV. Each arc has 35 FODO cells with sextupole magnets in each main cell, whereas each straight section has two matching cells and there are 10 cells in the straight section. One straight section contains 2 T and 8.1 m long wiggler magnet which is based on the wiggler design of CLIC [24]. A cell contains two 5.31 m long dipoles located between quadrupoles with 30 cm length. The chromaticity is controlled by two families of 20 cm long sextupoles. The

total circumference turns out to be 2908 m and the general parameters of the ring can be seen in Table 7. A scan has been performed to determine the optimum phase advances in terms of the emittance. Accordingly, $\mu_x, \mu_y = 0.363/2\pi, 0.1/2\pi$ are chosen for achieving minimum emittance. For the phase advance in the straight section, it is planned to be chosen around 90 degree to provide minimum beta function with maximum efficiency for injection and extraction elements.

Table 7: General parameters of the alternative PBR at injection and extraction energies, respectively.

Parameters	Values (inj./ext.)
energy	6 / 20 GeV
circumference	2908 m
equilibrium emittance	0.19 / 4.88 nm
energy loss/turn	1.12 / 57.8 MeV
natural chromaticity (h/v)	-69 / -123
hor. damping times	0.096 / 0.006 s

Dynamic aperture (DA) calculations, according to the tracking results of MADX-PTC [25], gives around 7 mm in horizontal and vertical directions.

BOOSTER

The last stage of the FCC-ee injector chain is a 98 km full energy injector housed in the same tunnel as the collider. This rapid cycling booster synchrotron is designed to ramp the beam energy up from 20 GeV to the beam energy of the collider in the range of 45.6 to 182.5 GeV and provide top-up injection every 5.6 to 51.74 seconds.

The booster will follow the footprint of the FCC hadron collider, while the collider rings are placed about 1.2 m on the outside. In the experimental cavern the collider's interaction region layout with crossing angle and local chromaticity compensation creates an offset of the interaction point of about 11 m, which leaves sufficient space for the booster to bypass the detector on the inside.

The magnetic lattice is of FODO structure. Two optics are used for the collider. First, a $90^\circ/90^\circ$ optics has been chosen for the operation at 120 GeV and 182.5 GeV. Secondly, a $60^\circ/60^\circ$ optics are designed for the operation at the lower beam energies 45.5 and 80 GeV, since this optics provides larger momentum compaction factor for longer bunches to mitigate the microwave instability [26]. The horizontal emittance evolution of each collider staging and the corresponding optics have been summarised in Table 8. In the arcs the cell length is about 54 m driven by the required horizontal equilibrium emittance. A comparison of the emittance values of booster and collider is given in Table 2. In the straight sections the cell length is 50 m except in the straight sections with the RF installation, where the cell length has been increased to create more room for the cryomodules. 566 m long section with smaller curvature at the beginning and at the end of each arc have been designed to house the

Table 8: Horizontal equilibrium emittances of the booster compared to the values of the collider for all four beam energies. The 60° optics is used for 45.5 GeV and 80 GeV operations while the 90° optics will be used for 120.0 GeV and 182.5 GeV.

beam energy (GeV)	booster emittance (nm)	collider emittance (nm)
45.5	0.24	0.24
80.0	0.73	0.84
120.0	0.55	0.63
182.5	1.30	1.48

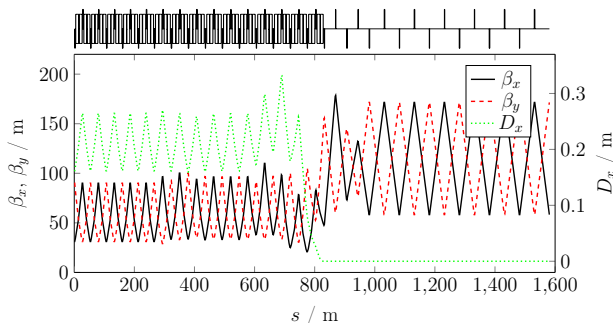


Figure 12: Beta functions and horizontal dispersion function of the transition from the arc lattice into a straight section with RF installation. The first five cells are regular arc FODO cells with a length of 54 m. The following section of 566 m consists of ten FODO cells with different bending angle to fit the geometry of the dispersion suppressor of the hadron collider. They also serve as quadrupole-based dispersion suppressor and matching section to the optics of the straight FODO cells with 100 m length.

dispersion suppressor of the FCC hadron collider. In these sections, the cell length is 56.6 m and a quadrupole-based dispersion suppressor scheme was chosen for the booster. Figure 12 shows the betafuncions in the transition of the periodic solution of arc 2 via the FCC-hh dispersion suppressor section into the straight section with the RF installation [27].

At 20 GeV beam energy the horizontal equilibrium emittance shrinks down to only $\epsilon_x = 15$ pm with the $90^\circ/90^\circ$ optics. As a consequence intra-beam scattering would blow up the emittance blow-up of a factor 48. In addition, the transverse damping time is $\tau_x = 10$ s, which would not allow to reach the equilibrium before the ramp-up. Therefore, 16 wiggler magnets are installed at the beginning and at the end of the straight sections with the RF system. The damping time is decreased $\tau_x = 0.1$ s and the horizontal equilibrium emittance is increased to $\epsilon_x = 300$ pm and $\epsilon_x = 296$ pm for the $60^\circ/60^\circ$ optics and the $90^\circ/90^\circ$ optics respectively. The wigglers have a length of $L_w = 9.1$ m with a period length of $\lambda_w = 0.23$ m. The wiggler have been chosen to be normal-conducting as they have to be switched off during the

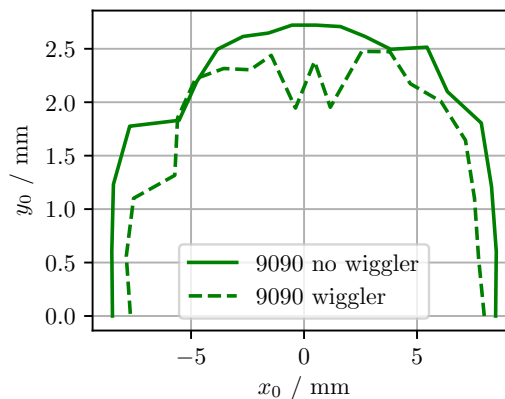


Figure 13: Dynamic aperture of the FCC-ee booster with $90^\circ/90^\circ$ optics at 20 GeV beam energy with and without wiggler magnets for a beta-function of 100 m.

energy ramp-up. Otherwise the energy loss by synchrotron radiation would exceed the capacities of the RF system. The pole tip field is $B = 1.8$ T, the actual wiggler field is then $B_w = 1.45$ T. The characteristics of the synchrotron radiation light fan created by the wigglers is currently under investigation by the vacuum group.

From the different sextupole schemes that were studied a non-interleaved sextupole scheme provided the largest DA for both optics. Tracking studies showed that the wigglers do not decrease the dynamic aperture significantly as shown in Fig. 13. The DA was determined by the survival of the particles after 1000 turns.

CONCLUSION

The RF-gun is ready for prototyping and positron study is continuing. The linacs up to 20 GeV (except 1.54 GeV positron linac part) have been finalized. They promise a nearly perfect transmission with low emittance to be safely injected into the pre-booster or booster. All in all, linac consists of 318 meters S-Band to reach 6 GeV, and 488 m C-Band to reach additional 14 GeV acceleration.

The damping wiggler and Robinson wiggler magnets will be inserted into the SPS lattice. The insertion of both type of wigglers will lead SPS to reach at the targeted equilibrium emittance with an acceptable energy loss per turn. The DA optimization for alternative pre-booster and simulations of Robinson wiggler for SPS are ongoing. The DA of top-up booster is fairly enough for safe acceptance of the beam from pre-boosters or C-Band linac. Additionally, final 6D tracking studies including wigglers and transverse quadrupole misalignments are under way. The instability study of the booster, such as microwave and transverse mode coupling instabilities, is also ongoing.

Each of the FCC-ee injectors has been designed with alternative options. The injector baseline satisfies all requirements, even with large safety margins. In particular, it supports the proposed bootstrapping injection mode of

the collider. With the proposed injector, the collider can be filled from zero in about 17 minutes at the Z pole, and even much faster at higher energies. The bunch schedules have been optimized for maximum average luminosity in operation.

REFERENCES

- [1] K. Oide *et al.*, "Design of beam optics for the future circular collider e^+e^- collider rings", *Phys. Rev. Accel. Beams*, vol. 19, p. 111005, Nov. 2016.
- [2] S. Ogur *et al.*, "Bunch Schedules for the FCC-ee Pre-injector", Proceedings of Int. Particle Accelerator Conf. (IPAC'18), Vancouver, Canada, Apr.-May 2018, MOPMF001.
- [3] A. V. Andrianov *et al.*, "Development and low power test of the parallel coupled accelerating structure", *JINST* 11 P06007, 2016.
- [4] Y. D. Chernousov *et al.*, "Accelerating structure with parallel connection". Patent for invention (Russia), No. RU2472244C1, BI. 01/10/2013, № 1.
- [5] I. Chaikovska *et al.*, "Experimental Activities on High Intensity Positron Sources Using Channeling", *Proceedings of IPAC'17*, Copenhagen, Denmark, WEPIK002, 2017.
- [6] P. Martyshkin, "Preliminary result of FCC positron source simulation", CERN, Geneva, Switzerland, accessed in September 2018, <https://indico.cern.ch/event/623025/contributions/2576145/attachments/1452960/2241145/Presentation2.pdf>
- [7] I. Chaikovska *et al.*, "Positron source", talk presented at the FCC-week 2017, Berlin, Germany, accessed in March 2018, https://indico.cern.ch/event/556692/contributions/2590440/attachments/1468997/2272259/e_FCCweek2017_IC.pdf
- [8] P. Martyshkin, "FCC-ee Flux Concentrator Computer Models", CERN, Geneva, Switzerland, accessed in September 2018, <https://indico.cern.ch/event/749013/contributions/3098680/attachments/1699198/2735883/FCC-FC.pdf>
- [9] N. Iida *et al.*, "Beam Dynamics in Positron Injector Systems for the Next Generation b-Factories", *Proceedings of IPAC 2011*, THYA01, San Sebastian, Spain, 2011.
- [10] S. Ogur *et al.*, "Layout and Performance of the FCC-ee Pre-injector Chain", Proceedings of Int. Particle Accelerator Conf. (IPAC'18), Vancouver, Canada, Apr.-May 2018, MOPMF034.
- [11] K. Yokoya, "Short-Range Wake Formulas for Infinite Periodic Pill-Box", 1998.
- [12] T. K. Charles, et al. "Bunch Compression and Turnaround Loops in the FCC-ee Injector Complex," 9th International Particle Accelerator Conference IPAC2018, Vancouver, BC, Canada, 2018, THPAF037, 3044-3047.
- [13] D. Douglas, "Suppression and Enhancement of CSR-Driven Emittance Degradation in the IR-FEL Driver," *Technical Report JLAB-TN-98-012*, 1998.
- [14] S. Di Mitri, M. Cornacchia, and S. Spampinati, "Cancellation of coherent synchrotron radiation kicks with optics balance," *Phys. Rev. Lett.*, 110, 014801, 2013.
- [15] S. Di Mitri and M. Cornacchia, "Electron beam brightness in linac drivers for free-electron-lasers," *Phys. Rep.*, 539, 2014.
- [16] R. Hajima, "A first-order matrix approach to the analysis of electron beam emittance growth caused by coherent synchrotron radiation," *Japanese Journal of Applied Physics, Part 2: Letters*, 42, pp. 974-976, 2003.
- [17] Y. Jiao, X. Cui, X. Huang, and G. Xu, "Generic conditions for suppressing the coherent synchrotron radiation induced emittance growth in a two-dipole achromat," *Phys. Rev. STAB*, 17, 060701, 2014.
- [18] Y. Papaphilippou *et al.*, "Design Guidelines for the Injector Complex of the FCC-ee", in *Proc. 7th Int. Particle Accelerator Conf. (IPAC'16)*, Busan, Korea, May 2016, paper THPMR042, pp. 3488-3491, ISBN: 978-3-95450-147-2, doi:10.18429/JACoW-IPAC2016-THPMR042.
- [19] O. Etisken *et al.*, "Pre-Booster Ring Considerations for the FCC e^+e^- Injector", in *Proc. 9th Int. Particle Accelerator Conf. (IPAC'18)*, Vancouver, BC, Canada, Apr. 4, pp. 83-86, doi:10.18429/JACoW-IPAC2018-MOPMF002.
- [20] Y. Papaphilippou *et al.*, "The SPS as an Ultra-Low Emittance Damping Ring Test Facility for CLIC", in *Proc. 4th Int. Particle Accelerator Conf. (IPAC'13)*, Shanghai, China, May 2013, paper TUPME042, ISBN: 978-3-95450-122-9.
- [21] The LEP injector study group, "The LEP injector chain", in *LEP design report*, CERN-SPS/63-26, 1983.
- [22] Y. Baconnier *et al.*, "Emittance Control of the PS e^+e^- Beams Using a Robinson Wiggler", *Nuclear Instrument and Methods in Physics Research A234* (1985) 244-252, North-Holland, Amsterdam, 1984.
- [23] T. Goetsch *et al.*, "Status of the Robinson Wiggler Project at the Metrology Light Source", in *Proc. 6th Int. Particle Accelerator Conf. (IPAC'15)*, Richmond, VA, USA, May 2015, pp. 132-134, doi:10.18429/JACoW-IPAC2015-MOPWA019.
- [24] F. Antoniou, "Optics Design of Intrabeam Scattering Dominated Damping Rings", CLIC Note 989, CERN-Thesis-2012-368.
- [25] CERN-BE/ABP Accelerator Beam Physics Group, MAD-Methodical Accelerator Design. <http://mad.web.cern.ch/mad/>
- [26] E. Belli *et al.*, "Single Bunch Instabilities in FCC-ee", in Proceedings of IPAC2018, Vancouver, BC, Canada, pp. 3336-3339.
- [27] B. Harer *et al.*, "Status of the FCC-ee Top-Up Booster Synchrotron", Proceedings of Int. Particle Accelerator Conf. (IPAC'18), Vancouver, Canada, Apr.-May 2018, MOPMF059.